RESEARCH ARTICLE

Differential secretome analysis of cancer-associated fibroblasts and bone marrow-derived precursors to identify microenvironmental regulators of colon cancer progression

Astrid De Boeck[1], An Hendrix[1], Dawn Maynard[2], Mieke Van Bockstal[3], Annick Daniëls[4], Patrick Pauwels[5], Christian Gespach[6], Marc Bracke[1] and Olivier De Wever[1]

[1] Laboratory of Experimental Cancer Research, Department of Radiation Oncology and Experimental Cancer Research, Bethesda, MD, USA
[2] Medical Genetics Branch, National Human Genome Research Institute, Bethesda, MD, USA
[3] Department of Pathology, Ghent University Hospital, Ghent, Belgium
[4] Laboratory of Experimental Hematology, Jesse Hospital, Hasselt, Belgium
[5] Department of Pathology, University of Antwerp, Wilrijk, Belgium
[6] INSERM UMR_S938, Molecular and Clinical Oncology, Université Paris VI Pierre et Marie Curie, Centre de Recherche Saint-Antoine, Paris, France

Received: May 2, 2012
Revised: October 29, 2012
Accepted: November 8, 2012

The identification of cancer-associated fibroblast (CAF)-derived proteins that mediate interactions between the tumor stroma and cancer cells is a crucial step toward the discovery of new molecular targets for therapy or molecular signatures that improve tumor classification and predict clinical outcome. CAF are α-smooth muscle actin positive, representing a myofibroblast phenotype that may differentiate from multiple precursor cells, including bone marrow-derived mesenchymal stem cells (MSC). Transforming growth factor-β1 (*TGF-β1*) is a crucial inducer of α-smooth muscle actin positive CAFs. In this study, we aimed to identify CAF-derived regulators of colon cancer progression by performing a high-throughput differential secretome profiling between CAF compared to noncancer-activated bone marrow-derived MSC. In addition, we explored the effect of TGF-β1 on the secretion of proteins by bone marrow-derived MSC in comparison with the protein secretion profile of CAF. TGF-β1 induced de novo secretion of 84 proteins in MSC, of which 16 proteins, including stromal-derived factor-1α and Rantes, were also present in CAF secretome. Immunohistochemistry further validated the expression of selected candidates such as tenascin C, fibronectin ED-A domain and stromal-derived factor-1 in clinical colon cancer specimens. In conclusion, this differential secretome approach enabled us to identify a series of candidate biomarkers for colon cancer that are associated with a CAF-specific phenotype.

Correspondence: Dr. Olivier De Wever, Laboratory of Experimental Cancer Research, Department of Radiotherapy and Nuclear Medicine, Ghent University Hospital, De Pintelaan 185, B-9000 Gent, Belgium
E-mail: olivier.dewever@ugent.be
Fax: +32-9-3324991

Abbreviations: α-SMA, α-smooth muscle actin; **CAF**, cancer-associated fibroblasts; **CM**, conditioned medium; **ECM**, extracellular matrix; **ED-A Fn**, ED-A fibronectin; **HGF**, hepatocyte growth factor; **IHC**, Immunohistochemistry; **MMP**, matrix metalloproteinase; **MSC**, mesenchymal stem cells; **SDF-1**, stromal-derived factor-1; **SPARC**, secreted protein acidic and rich in cysteine; **TGF-β1**, transforming growth factor β1; **TIMP**, tissue inhibitor of metalloproteinase; **TNC**, tenascin C

Colour Online: See the article online to view Figs. 1–5 in colour.

Keywords:
Cancer-associated fibroblasts / Cell Biology / Colon cancer / Mesenchymal stem cells / MS / Secretome

Additional supporting information may be found in the online version of this article at the publisher's web-site

1 Introduction

Colorectal cancer is the third most common cancer accounting for 9% of cancer deaths [1]. Because mortality from colorectal cancer is often due to distant metastasis, there is an urgent need to identify prospective biomarkers for early detection. The development of an altered stromal microenvironment in response to carcinoma is an early event during carcinogenesis and a prerequisite for tumor invasion and metastasis [2]. The most common marker of reactive stroma is the appearance of activated cells with myofibroblast characteristics, so called cancer-associated fibroblasts (CAF), identifiable by their expression of α-smooth muscle actin (α-SMA) [3]. CAF are master regulators of paracrine signaling driving progression of various cancers through release of soluble factors and extracellular matrix (ECM) remodelling [3]. Diverse evidence shows that cancer cell-secreted factors, such as transforming growth factor-β1 (TGF-β1), are responsible for initiating and maintaining the myofibroblast phenotype in precursor cells [4, 5]. Bone marrow-derived mesenchymal stem cells (MSC) develop myofibroblast characteristics in response to TGF-β1 [6] and localize to solid tumors after intravenous administration in animal models [7, 8]. In an ovarian cancer model, bone marrow-derived MSC were shown to ultimately lead to an enhancement of tumor growth via differentiation into myofibroblasts, which supported angiogenesis and tumor growth [9]. Recently, we described that MSC promote colorectal cancer progression through paracrine neuregulin 1(NRG1)/HER3 signaling, which was further induced by TGF-β1 [10]. These results support the active contribution of MSC as precursors of CAF during tumor progression and emphasize the reciprocal tumor-stromal cross-talk.

Understanding the molecular changes within the tumor microenvironment is relevant not only for discovering potential therapeutic targets, but also for identifying putative molecular signatures and biomarkers that may improve tumor classification and predict clinical outcome. Several approaches have been used to address the stromal response to invasive cancer growth, including gene and protein expression profiling of microdissected reactive stroma or primary stromal cell cultures [11–14]. Considering the key role of soluble factors in mediating intercellular interactions through autocrine and paracrine signaling, the "secretome" originating from classical, nonclassical, and exosomal protein secretion mechanisms [15, 16], is therefore a potential source of a novel family of cancer biomarkers.

In this study, we compared the secretome of colon CAF versus naive bone marrow-derived MSC and investigated the effect of recombinant TGF-β1 on myofibroblast differentiation and protein secretion in MSC. This differential secretome approach uncovers autocrine/paracrine components in the modulation of cancer-stroma interactions and identifies a series of putative biomarkers that are associated with an activated stromal cell phenotype.

2 Material and methods

2.1 Cell culture

Human MSC were isolated from sternal bone marrow aspirates obtained in two noncancer patients before cardiac surgery, as described [17]. MSC were analyzed flow cytometrically after every passage and presented the characteristic signature of mesenchymal stem cell surface markers [18, 19] (Supporting Information Material and methods and Supporting Information Fig. 1). MSC were cultured on high-extension silicone rubber dishes with a stiffness of 5 kPa (ExCellness Biotech SA, Ecublens, Switzerland) [20].

Human CAF were isolated from colon cancer tissue in two patients with colon adenocarcinoma, submitted to surgical resection for therapeutic purposes. Tissue fragments were cut in small pieces (2–3 mm^3) and transferred into a 6-well plate with 100 μL of FBS supplemented with antibiotics added on top of each fragment. Cultures were incubated at 37°C with 10% CO_2 in air for 24 h. After 24 h, Dulbecco's modified Eagle's medium with low glucose (LG-DMEM) (Invitrogen, Carlsbad, CA) containing 10% FBS was added into each well. Cell outgrowth was observed after 3–6 days. After 15 days, adherent cells were transferred to a 25-cm^2 tissue culture flask by trypsinization with a trypsin-EDTA (0.25% – 1 mM) solution (Invitrogen). CAF and MSC were incubated in LG-DMEM containing 10% FBS, penicillin (100 U/mL) and streptomycin (100 μg/mL) (Invitrogen) at 37°C with 5% CO_2 in air. Medium was refreshed twice weekly.

Green fluorescent protein (peGFP-C1; Clontech, BD Biosciences) overexpressing HCT-8/E11 cells [10] (HCT-8/E11-GFP) were generated by electroporation (Cell line nucleofector kit V, Lonza, Basel, Switzerland) and stable cell lines were selected in G418 (1 mg/mL). HCT-8/E11(-GFP) cells were maintained in DMEM (Invitrogen) supplemented

with 10% FBS and antibiotics (penicillin/streptomycin), and incubated at 37°C with 10% CO_2 in air.

2.2 Induction of adipogenic, osteogenic, and myofibroblast differentiation

Cells were tested by their capacity to differentiate into adipocytes and osteocytes with use of a functional identification kit (R&D Systems, Minneapolis, MN). MSC were treated with rTGF-β1 (10 ng/mL; R&D Systems) for 6 days to induce myofibroblast differentiation.

2.3 Antibodies

A summary of the antibodies used for Western blot analysis and immunohistochemistry (IHC) is presented in Supporting Information Table 1.

2.4 Preparation of CM

A total of 2×10^6 cells were washed three times with 10 mL of serum-free LG-DMEM and incubated at 37°C with 20 mL serum-free LG-DMEM for 48 h. The conditioned medium (CM) was harvested, centrifuged at 1250 g for 5 min at 4°C and passed through a 0.22-μm filter. CM was stored at −20°C, a procedure that did not alter its activity as tested with 6-month-old medium. The CM was concentrated in centriprep tubes YM-3 (Amicon, Millipore Corp., Bedford, MA), sterilized, and diluted with fresh serum-free LG-DMEM: 0.5 mL CM contained soluble factors derived from 5×10^5 cells. For Western blotting and LC-MS/MS analysis, CM was further concentrated such that 25 μL CM contained soluble factors derived from 2×10^5 cells.

2.5 Multicellular spheroid collagen invasion assay

A heterotypic spheroid collagen invasion assay was performed as described previously [21]. Briefly, a bottom gel layer of collagen type I solution was mixed with 10^6 MSC, rTGF-β1-treated MSC or CAF and gelified. HCT-8/E11-GFP spheroids with a diameter of ± 150 μm were mixed with collagen type I solution and gently poured on the preformed collagen type I gel layer. At 0, 24, and 48 h bright field and GFP-fluorescent images were made of 10 preselected spheroids on a Zeiss Axiovert 200 M fluorescence microscope (Carl Zeiss MicroImaging GmbH, Göttingen, Germany). Phase-contrast images were converted to binary images using ImageJ software and the projected surface area was quantified. After 96 h, collagen matrices were fixed in 3% paraformaldehyde for 10 min and phalloidin-TRITC (Sigma-Aldrich) staining as described [21]. Spheroids were imaged with a Zeiss 510 META confocal laser-scanning microscope (Carl Zeiss, Micro-imaging Inc., Heidelberg, Germany). All the images shown are collapsed z-stacks.

2.6 LC-MS/MS analysis and bioinformatics

LC-MS/MS analysis was performed in two independent gel assays using concentrated CM from different MSC and CAF populations. A 25 μL of concentrated CM was run on NuPAGE 4–20% Bis–Tris gradient gels (Invitrogen) in denaturating SDS buffer, stained with 0.5% Coomassie Brilliant Blue (Bio-Rad, Hercules, CA) in 40% methanol and 10% acetic acid, and destained in a solution composed of 40% methanol and 10% acetic acid. Gel bands were processed and analyzed by LC-MS/MS as previously described [22]. Raw MS/MS files were submitted to the NIH MASCOT Cluster [23] using MASCOT DAEMON version 2.2. Data were searched against the UNIPROT-SPROT database, updated on 20/05/08, as described [22]. Only peptides that were detected in two separate experiments were considered. If only 1 peptide was detected, only proteins with more then 10% coverage were retained. Peptide identifications from one representative experiment are shown. A more detailed description of the LC-MS/MS analysis is given in Supporting Information Material and methods.

Each protein was assigned to the functional classification based on the gene ontology (GO) annotation system using the DAVID database bioinformatics resources (http://david.abcc.ncifcrf.gov) (36). In addition, we used Ingenuity Pathway Analysis software (http://www.ingenuity.com/) to determine biological functions and diseases that were associated with the defined protein set. An area-proportional Venn diagram was constructed using BioVenn (http://www.cmbi.ru.nl/cdd/biovenn/).

2.7 Western blot analysis, antibody arrays, and ELISA assays

For Western blotting, 20 μL of concentrated CM was diluted in 10 μL reducing Laemmli lysis buffer (0.125M Tris-HCl (pH = 6.8), 10% glycerol, 2.3% SDS) and boiled for 5 min at 95°C. For the detection of phosphorylated c-Met (p-c-Met), HCT-8/E11 cells were grown at 70% confluence and treated for 15 min as indicated. Cells were harvested with Laemmli lysis buffer and boiled for 5 min at 95°C. Samples were run on NuPAGE 4–20% Bis–Tris gradient gels (Invitrogen), transferred to polyvinylidene fluoride membranes, blocked in 5% nonfat milk in PBS or 4% BSA in PBS for phosphorylated proteins with 0.5% Tween-20, and immunostained. A human angiogenesis antibody array, human chemokine antibody array, human matrix metalloproteinase (MMP) antibody array, and human growth factor antibody array (RayBiotech Inc., Norcross, GA) were used according to the manufacturer's protocol. Human hepatocyte growth factor (HGF) and stromal-derived factor-1 (SDF-1α) ELISA assays were from

R&D Systems. ELISA assays were performed in two independent assays using different MSC and CAF populations. The data are expressed as mean and standard error from one representative experiment performed in quadruplicate.

2.8 Immunohistochemistry

IHC for tenascin C (TNC), ED-A fibronectin (ED-A Fn), and α-SMA was performed on paraffin embedded primary colon cancer tissues ($n = 5$), collected at Ghent University Hospital, in accordance with local ethics committees. Specimens were fixed in a 4% formaldehyde solution for 12–48 h and embedded in paraffin. IHC was performed on 3.5-μm tissue sections on Superfrost slides (Menzel-Gläser, Braunschweig, Germany) using a Ventana Automated Slide Stainer (Benchmark XT, Ventana Medical Systems Inc., Arizona, USA), according to manufacturer's instructions. Heat-induced epitope retrieval was carried out, using Cell Conditioning 1 for α-SMA, and using Cell Conditioning 2 for ED-A Fn. No pretreatment was used during the staining procedure for TNC. For all antibodies, visualisation was achieved with the ultraView™ Universal DAB Detection Kit (Ventana Medical Systems Inc., Arizona, USA).

SDF-1 and α-SMA IHC were performed on frozen sections ($n = 5$) collected at University Hospital Antwerp, in accordance with local ethics committees. Frozen sections were fixed with cold acetone for 10 min and incubated with anti-SDF-1α or anti-α-SMA for 1 h at room temperature in a humidified chamber. After washing with PBS, all sections were incubated with a biotinylated goat anti-rabbit or anti-mouse secondary antibody at room temperature for 45 min, followed by incubation with streptavidin-biotin peroxidase solution. Color reaction was developed in diaminobenzidine solution, and counterstaining was performed with Mayer's hematoxylin solution.

Protein expression was evaluated by light microscopy. The extent of TNC, ED-A Fn, and SDF-1α staining was scored by assigning the percentage of α-SMA stained CAF (no staining; mild: < 30% positive staining; moderate to high: > 30% positive staining).

2.9 Statistical analysis

Statistical calculations were performed using MedCalc (Version 11.0; MedCalc Software, Mariakerke, Belgium). Comparisons were performed using a two-sided repeated measures ANOVA test followed by a Student's *t*-test at individual time points for the area in the heterotypic spheroid collagen invasion assays and a two-sided unpaired Student *t*-test following D'Agostino–Pearson testing for normal distribution for ELISA analysis. Data presented are representative of at least two independent experiments and are expressed as mean and standard error. *p* values less than 0.05 were considered to be statistically significant.

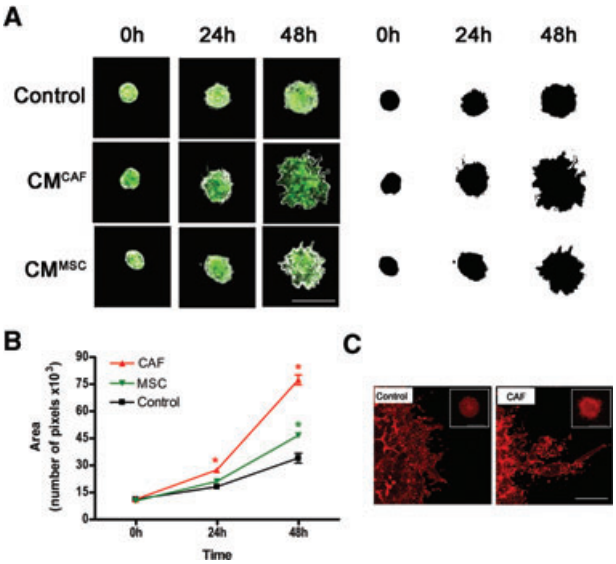

Figure 1. (A) Combined bright-field and GFP-fluorescence images of a representative HCT-8/E11-GFP spheroid followed at different time intervals under control and CAF or MSC coculture conditions. Scale bar, 200 μm (left panel). Computerized binary image processing of GFP-phase contrast picture using ImageJ software (right panel). (B) Image J-assisted calculation of the projected surface area from HCT-8/E11-GFP spheroids followed at different time intervals under control and CAF or MSC coculture conditions. Results are expressed as mean and standard error from six spheroids for each condition. *$p < .01$. (C) Confocal images of a typical invasion front from a phalloidin-Alexa Fluor 594 stained HCT-8/E11-GFP spheroid cultured for 96 h under control or CAF coculture conditions. Scale bar, 50 μm; inset shows whole spheroid, scale bar, 300 μm.

3 Results

3.1 Pro-invasive growth effect of naive MSC and CAF on HCT-8/E11-GFP cells

To investigate the proinvasive growth effect of soluble factors from naive MSC or CAF on colon cancer cells, heterotypic collagen invasion experiments were performed without physical contact between the spheroids and CAF or MSC. HCT-8/E11-GFP spheroids in coculture with MSC or CAF demonstrated a higher increase in projected surface area compared to controls (Fig. 1A and B; $p < 0.001$ for CAF and $p = 0.013$ for MSC). At 48 h, the spheroid area was twofold and 1.4-fold higher under CAF and MSC coculture, respectively, than the controls ($p < 0.001$ for CAF and $p = 0.003$ for MSC). Investigation of the F-actin organisation by confocal microscopy revealed that the control spheroids had smooth edges with occasional invasive extension formation (Fig. 1C, left panel), whereas the spheroids in coculture had an irregular perimeter with individual and collective cells invading the surrounding collagen matrix, as shown in Fig. 1C (right panel) for the CAF coculture.

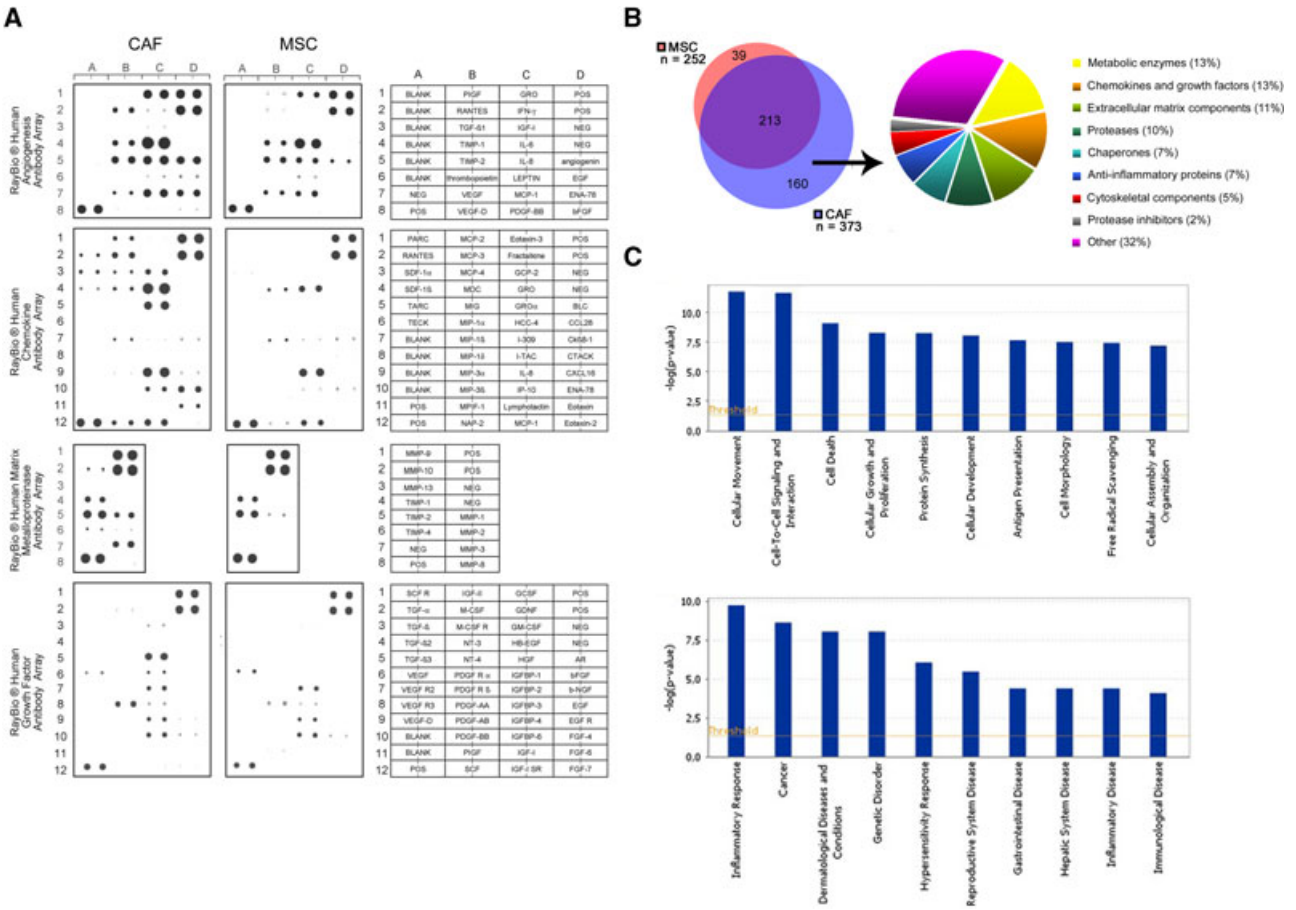

Figure 2. Differential protein secretome analysis in CAF and MSC. (A) Four antibody microarrays were used to identify differentially secreted proteins in CAF and MSC. Each protein is spotted horizontally in duplicate according to their identification name on the right panel. (B) An area-proportional Venn diagram visualizes the distribution of unique and common proteins secreted in CAF and MSC using antibody arrays and LC-MS/MS (left panel); pie chart for the distribution of proteins that were only secreted by CAF ($n = 161$) according to their functional category (DAVID database) (right panel). For each category, the percentage of proteins included is reported. (C) Top 10 biological functions (upper panel) and diseases (lower panel) that were significantly associated with the proteins that were only secreted by CAF ($n = 161$). The negative log of the *p*-value is shown on the *y*-axis. Diagram generated through Ingenuity Pathway Analysis software.

3.2 Differential secretome analysis

We performed LC-MS/MS analysis to identify differentially secreted proteins between CAF and MSC. Since highly bioactive proteins such as growth factors, chemokines or ECM-processing proteases are often secreted at very low levels and usually not detected by gel-electrophoresis-based proteomics [24], we supplemented our LC-MS/MS with four different antibody arrays based on growth factors, chemokines, MMPs, and angiogenesis markers (Fig. 2A). All proteins identified are summarized in Supporting Information Table 2. Altogether, 367 and 252 proteins were identified in CM^{CAF} and CM^{MSC}, respectively. A Venn diagram shows the distribution of unique and shared proteins for the two sets of CM (Fig. 2B, left panel). We observed that 39 (9.6%) and 154 (37.9%) proteins were uniquely secreted by MSC and CAF, respectively, while 213 proteins (52.5%) were detected in both CM samples. Unique proteins released by CAF were clustered in nine functional categories according to their biological functions, morphological criteria and cellular components using the DAVID functional annotation tool. These included ECM components (e.g. TNC and several laminin subunits [α2, α4, and α5]), proteases (e.g. MMP-2, MMP-3, cathepsin H), anti-inflammatory/anti-oxidant proteins (e.g. granulocyte chemotactic protein-2 [GCP-2 and eotaxin), cytoskeletal components (e.g. actin-related proteins), metabolic enzymes (f.e. different proteasome subunits), chemokines and growth factors (e.g. SDF-1α, HGF and epidermal growth factor), protease inhibitors (e.g. tissue inhibitor of metalloproteinase (TIMP-4) and angiotensinogen), chaperone proteins (e.g. calreticulin), and others (Fig. 2B, right panel). The two major biological functions associated with this set of proteins were regulation of cellular movements and cell-to-cell signaling and interactions (Fig. 2C, upper panel). Corresponding

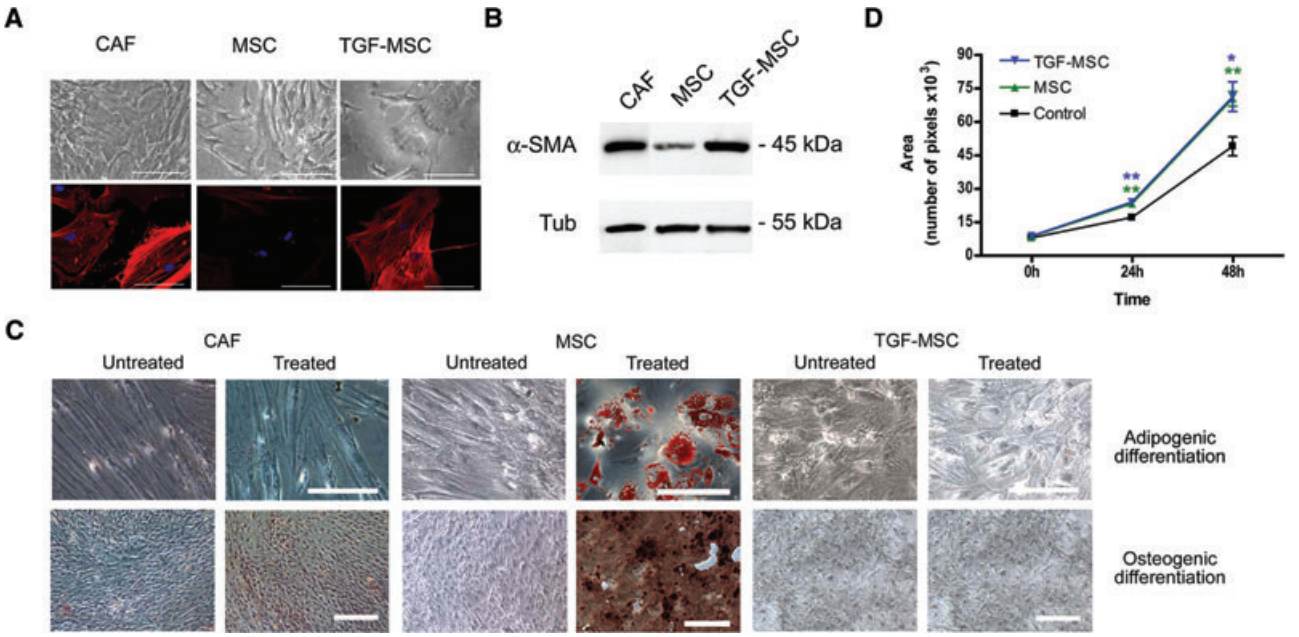

Figure 3. Effect of rTGF-β1 on α-SMA expression, multipotency and proinvasive growth properties in MSC. (A) Phasecontrast images (upper panel) and α-SMA immunofluorescence (lower panel) of MSC and rTGF-β1-treated-MSC and CAF. Scale bar, 100 μm. (B) Western blot evaluation of α-SMA expression in MSC, rTGF-β1-treated-MSC, and CAF. (C) MSC, rTGF-β1-treated-MSC, and CAF were investigated for their adipogenic and osteogenic differentiation potential in vitro. Accumulation of lipid droplets (indicating adipogenic differentiation) is demonstrated by staining with Oil red O. Osteogenic differentiation is indicated by calcium deposition as demonstrated by Alizarin red staining. (D) Image J-assisted calculation of the projected surface area from HCT-8/E11-GFP spheroids followed at different time intervals control and MSC or TGF-MSC coculture conditions. Results are expressed as mean and standard error from six spheroids for each condition. $^{**}p < 0.05$, $^{*}p < 0.01$. Abbreviations: rTGF-β1-treated-MSC, TGF-MSC. Scale bar, 200 μm.

diseases were inflammatory responses and cancer progression (Fig. 2C, lower panel).

3.3 Effect of TGF-β1 on α-SMA expression, multipotency, and proinvasive growth effect in MSC

To determine if MSC are potential precursors of CAF, we explored whether rTGF-β1 can induce α-SMA expression and loss of multipotency. Treatment with rTGF-β1 induced morphological changes (Fig. 3A, upper panel) and α-SMA positive stress fibers (Fig. 3A, lower panel) in MSC with a 2.8-fold increase in α-SMA protein expression levels, comparable to CAF (Fig. 3B). Upon 6 days of rTGF-β1 treatment, MSC almost completely lost their ability to differentiate into osteocytes and adipocytes, in contrast to control MSC. Similar to TGF-β1-treated MSC, CAF demonstrated minimal ability to differentiate into adipocytes and osteocytes (Fig. 3C). rTGF-β1-treated MSC significantly stimulated invasive growth of HCT-8/E11-GFP spheroids comparable to the effect of naive MSC (Fig. 3D).

Next, we analyzed the effect of rTGF-β1 on protein secretion in MSC and compared this altered secretome profile with that of CAF (Fig. 4A and Supporting Information Table 2). A Venn diagram visualises the distribution of unique and shared secretome proteins for CAF, MSC, and TGF-β1-treated MSC (Fig. 4B). rTGF-β1 induced de novo secretion of 84 proteins in MSC. Among them, 16 proteins were also identified in CM^{CAF}, and consisted mainly of chemokines and growth factors including SDF-1α, Rantes, TGF-β2, growth differentiation factor 15 (GDF-15), and granulocyte chemotactic protein-2 (Fig. 4B, right panel).

3.4 Validation of protein secretomes

Western blotting, ELISA and functional testing were performed for 11 selected candidates in order to confirm the LC-MS/MS and antibody array data (Fig. 4C, D, and E). Selected candidates belonged to critical functional proteins implicated in inflammation and cancer, i.e. proteases (MMP-3, Cathepsin D), growth factors (SDF-1α, HGF), the protease inhibitor TIMP-1 and ECM components (TNC, hyaluronan and proteoglycan link protein 1, Galectin-1, ED-A Fn, secreted protein acidic and rich in cysteine [SPARC]).

TNC, MMP3, and HGF were only detected in CM^{CAF}. Western blotting confirmed these results for MMP-3 and TNC (Fig. 4C). HGF was present at a concentration of 8.3 ± 0.4 ng/mL in CM^{CAF}, as measured by ELISA analysis

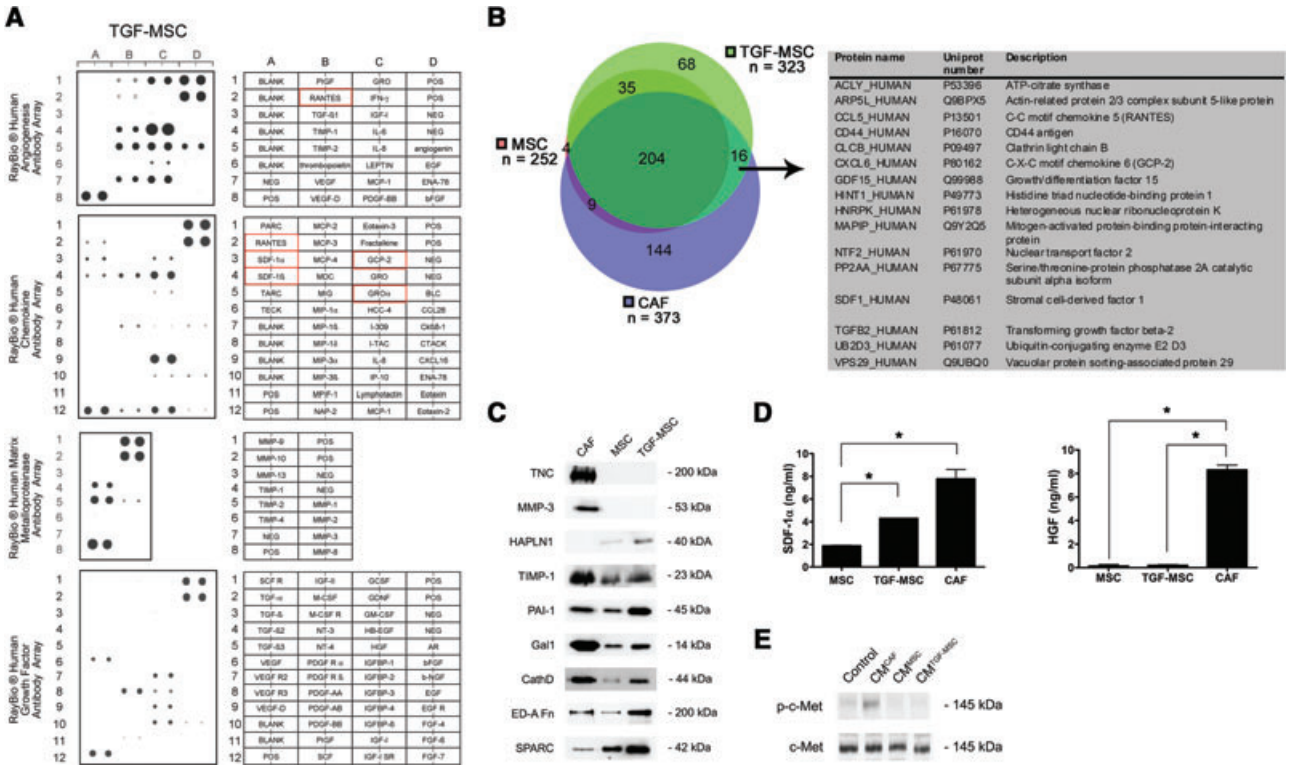

Figure 4. Effect of rTGF-β1 on protein secretion in MSC and validation of selected candidates. (A) Four antibody arrays were used to identify secreted proteins in rTGF-β1-treated MSC. Differentially secreted proteins in rTGF-β1-treated MSC versus MSC (see Fig. 1) are highlighted by red frames. (B) An area-proportional Venn diagram visualizes the differential distribution of unique and common secreted proteins in CAF, MSC, and rTGF-β1-treated MSC that were identified using antibody arrays and LC-MS/MS (left panel); description of de novo secreted proteins in rTGF-β1-treated MSC that that were common with CAF secretome (right panel). (C) Western blot analysis of selected candidates in CM^{CAF}, CM^{MSC}, or $CM^{rTGF\text{-}\beta1\text{-}treated.\ MSC}$. Representative blots for CM^{MSC} and CM^{CAF} obtained from two independent donors are shown. (D) Quantification of SDF-1α (left panel) and HGF levels (right panel) in CM^{CAF}, CM^{MSC}, or $CM^{rTGF\text{-}\beta1\text{-}treated\ MSC}$ using ELISA analysis. Results are expressed as mean and standard error from one representative experiment performed in quadruplicate. $*p < 0.01$. (E) Western blot evaluation of phosphorylated c-Met (p-c-Met) and total c-Met expression levels in HCT-8/E11 cells treated with control medium or CM^{CAF}, CM^{MSC}, and $CM^{rTGF\text{-}\beta1\text{-}treated\ MSC}$. Abbreviations: rTGF-β1-treated MSC, TGF-MSC.

(Fig. 4D, right panel), in accordance with previous results [4]. The functionality of HGF in CM^{CAF} was further demonstrated by its ability to phosphorylate c-Met in colon cancer cells, which was not the case for CM^{MSC} and $CM^{rTGF\text{-}\beta1\ treated\ MSC}$ (Fig. 4E). The presence of hyaluronan and proteoglycan link protein 1 in CM^{MSC} and $CM^{rTGF\text{-}\beta1\ treated\ MSC}$, was confirmed by Western blotting. SDF-1α was detected in both $CM^{rTGF\text{-}\beta1\ treated\ MSC}$ and CM^{CAF}. ELISA analysis detected low amounts of SDF-1α in CM^{MSC} (1.87 ± 0.04 ng/mL) with a twofold increase upon TGF-β1-treatment (4.3 ± 0.02 ng/mL), as compared to 8.7 ± 0.8 ng/mL in CM^{CAF} (Fig. 4D, left panel). The largest group of proteins were common between the different sets of proteins. Among them, plasminogen activator inhibitor-1, TIMP-1, Galectin 1, Cathepsin D, SPARC, and ED-A Fn were validated by Western blot analysis (Fig. 4C).

Three selected proteins identified in CM^{CAF} together with α-SMA were further validated by IHC in five colon cancer samples (Fig. 5). All samples showed α-SMA-expressing CAF, organized in a network of intersecting bundles. In five of five tumor specimens moderate to high expression of ED-A Fn was observed in α-SMA-expressing CAF. A fainter expression pattern was also observed in the epithelial cancer nests. In four of five and in three of five tumor specimens mild expression of TNC and SDF-1 was observed in the α-SMA-expressing CAF network.

4 Discussion

The identification of CAF-derived proteins mediating stroma-cancer cell interactions is a crucial step toward the discovery of new therapeutic targets or prognostic signatures. Phenotypically, CAF are myofibroblasts characterized by the expression of α-SMA [3, 5]. CAF arise from several mobilised cell types including tissue-resident MSC and fibroblasts, and distant invaders such as bone marrow-derived MSC and fibrocytes [6]. A comparison of the secretome of cell culture grown CAF versus naive bone marrow-derived MSC allows

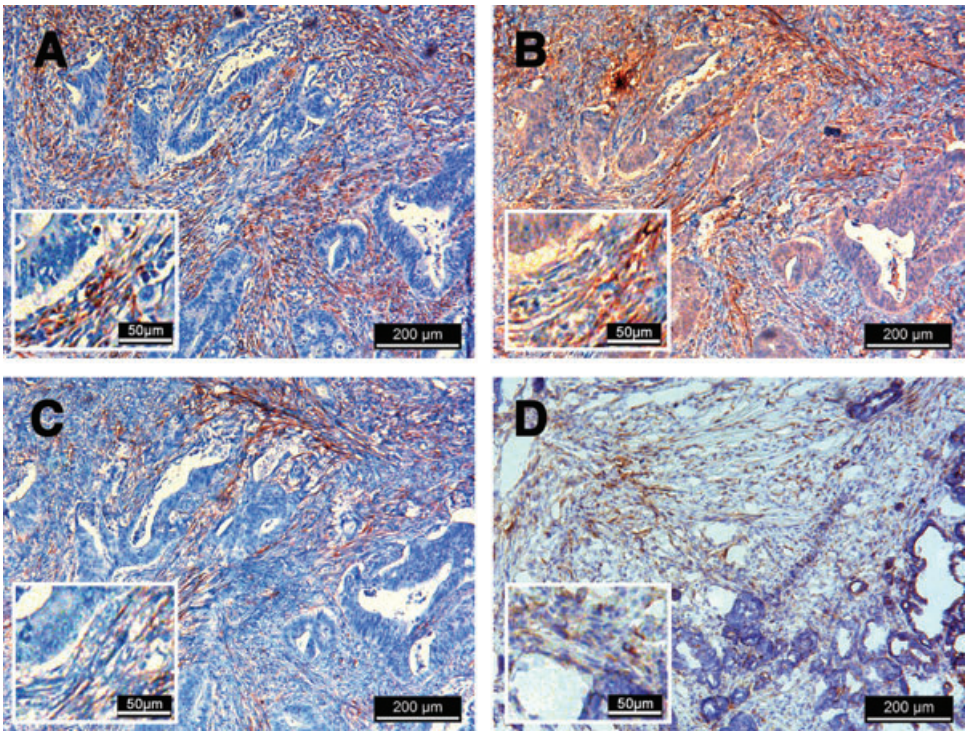

Figure 5. Immunohistochemical validation of selected candidates in clinical colorectal cancers. Human colon cancers were immunostained for (A) α-SMA and protein markers that were identified in CM^{CAF} including (B) ED-A Fn, (C) TNC and (D) SDF-1. Inset panels are higher magnification images. Representative examples are illustrated.

us to identify proteins that are uniquely secreted by cancer-activated stromal cells but not by their naive progenitor cells. Hundred fifty-four proteins were found to be differentially secreted by CAF versus MSC. This set of proteins was significantly associated with inflammatory response, cancer, cellular movement, and cell-to-cell signaling and interaction.

Mechanical resistance of the ECM, in conjunction with the action of TGF-β1, represents the main cues for myofibroblast differentiation and persistence in tumors [5]. We investigated the role of TGF-β1 in inducing the CAF phenotype in MSC. rTGF-β1 increased α-SMA expression, stress fiber organization and induced loss of multipotency. In agreement, rTGF-β1-treated MSC stimulated invasive growth of colon cancer cells, although to a lower level then CAF. Among the 84 de novo secreted proteins induced by rTGF-β1 in MSC, only 16 proteins were common with the CAF secretome. These results may indicate that additional factors act in cooperation with TGF-β1 to induce a fully differentiated MSC phenotype with increased proinvasive properties. TGF-β1-mediated signaling pathways are complex and highly context dependent, due to their extensive communications with other signaling pathways or mechanical force-induced signaling, leading to synergistic or antagonistic effects [5, 25, 26]. TGF-β1 induces chondrogenic differentiation in MSC in the presence of dexamethasone or 3D cell aggregates, demonstrating that the effects of rTGF-β1 on MSC differentiation depend on other microenvironmental factors [27, 28]. In addition, only a fraction of the CAF (20%) derives from MSC [8] and the CAF population represents a heterogeneous mixture of different subtypes [29], with their own genomic and secretomic fingerprint. We have to consider that our LC-MS/MS approach has mainly a qualitative value, since only differentially expressed proteins are identified in the rTGF-β1-treated-MSC group. However, Western blot validation revealed an increased expression of ECM proteins such as ED-A Fn and SPARC in rTGF-β1-treated-MSC compared to naive MSC, suggesting that aberrant secretion and not only de novo induction of these markers can be associated with MSC activation as well.

SDF-1, GDF-15, and CD44 are induced by TGF-β1 [30–32], in accordance with our results, and can be considered as reliable markers for CAF originating from the bone marrow. Interestingly, the CXCR4 ligand SDF-1 is induced in CAF after radiochemotherapy, which stimulates the recruitment of MSC from the bone marrow [33], and elevated SDF-1/CXCR4 levels correlate with poor survival in rectal cancer patients [34]. Karnoub et al. demonstrated that breast cancer cells stimulate de novo secretion of Rantes in MSC, which then acts in a paracrine fashion on cancer cell to enhance their motility, invasion and metastasis [7]. However, the cancer-cell-derived factor(s) that induced de novo Rantes secretion in MSC remained unexplored. TNC and HGF were only detected in CM^{CAF} and may therefore represent effectors and markers of CAF originating from resident fibroblasts. Previously, we have shown that phenotypically normal colon-derived fibroblasts secrete HGF and that rTGF-β1 treatment maintains HGF secretion and induces TNC secretion [4]. Interestingly, elevated TNC serum levels have been found in patients with metastatic colorectal cancers, compared with patients without metastases [35].

Rather few secretome profiles have been established by direct protein identification via mass spectrometry [36–39]. Interestingly, among 138 proteins detected by LC-MS/MS in the MSC secretome from two independent donors [39], 85 proteins were also identified in CM^{MSC} in our study, equating to a 62% overlap. Low abundance proteins are rarely detected by gel-based proteomics. Therefore, additional purification steps may be required. We previously identified rNRG-β1 in CM^{MSC} after heparin precipitation in order to sequester heparin-binding growth factors. NRG1 expression in MSC was further induced by rTGF-β1 and correlated with poor prognosis in colorectal cancer [10].

To our knowledge this is the first report presenting a large-scale analysis and identification of paracrine and autocrine factors that are secreted by CAF in comparison with bone marrow-derived mesenchymal precursor cells. Functional understanding of the factors regulating autocrine and paracrine signaling will support development of specific therapeutics and may unveil novel stroma-associated biomarkers.

This work was supported by the Intramural Research Program of the National Human Genome Research Institute, Centrum voor Gezwelziekten, the Scientific Exchange Program between the Flemish community and France (I.2007.03, T.2009.14, T.2010.14), INSERM (C. G.), Vlaamse Liga tegen Kanker (A. D. B and O. D. W), postdoctoral grant from Special Research Fund, Ghent University (A. H.), travel grant (A. H. and O. D. W.), a doctoral grant (A. D. B.), and a postdoctoral researcher (O. D. W. and A. H.) from Fund for Scientific Research-Flanders.

The authors have declared no conflict of interest.

5 References

[1] Siegel, R., Naishadham, D., Jemal, A., Cancer statistics. *CA Cancer J. Clin.* 2012, *62*, 10–29.

[2] De Wever, O., Mareel, M., Role of tissue stroma in cancer cell invasion. *J. Pathol.* 2003, *200*, 429–447.

[3] De Wever, O., Demetter, P., Mareel, M., Bracke, M., Stromal myofibroblasts are drivers of invasive cancer growth. *Int. J. Cancer* 2008, *123*, 2229–2238.

[4] De Wever, O., Nguyen, Q. D., Van Hoorde, L., Bracke, M. et al., Tenascin-C and SF/HGF produced by myofibroblasts in vitro provide convergent pro-invasive signals to human colon cancer cells through RhoA and Rac. *FASEB J.* 2004, *18*, 1016–1018.

[5] Hinz, B., Phan, S. H., Thannickal, V. J., Prunotto, M. et al., Recent developments in myofibroblast biology: paradigms for connective tissue remodeling. *Am. J. Pathol.* 2012, *180*, 1340–1355.

[6] De Boeck, A., Narine, K., De Neve, W., Mareel, M. et al., Resident and bone marrow-derived mesenchymal stem cells in head and neck squamous cell carcinoma. *Oral Oncol.* 2010, *46*, 336–342.

[7] Karnoub, A. E., Dash, A. B., Vo, A. P., Sullivan, A. et al., Mesenchymal stem cells within tumour stroma promote breast cancer metastasis. *Nature* 2007, *449*, 557–563.

[8] Quante, M., Tu, S. P., Tomita, H., Gonda, T. et al., Bone marrow-derived myofibroblasts contribute to the mesenchymal stem cell niche and promote tumor growth. *Cancer Cell.* 2011, *19*, 257–272.

[9] Spaeth, E. L., Dembinski, J. L., Sasser, A. K., Watson, K. et al., Mesenchymal stem cell transition to tumor-associated fibroblasts contributes to fibrovascular network expansion and tumor progression. *PloS One* 2009, *4*, e4992.

[10] De Boeck, A., Pauwels, P., Hensen, K., Rummens, J. L. et al., Bone marrow-derived mesenchymal stem cells promote colorectal cancer progression through paracrine neuregulin 1/HER3 signalling. *Gut.* 2012, doi: 10.1136/gutjnl-2011-301393.

[11] Finak, G., Bertos, N., Pepin, F., Sadekova, S. et al., Stromal gene expression predicts clinical outcome in breast cancer. *Nat. Med.* 2008, *14*, 518–527.

[12] Escher, N., Ernst, G., Melle, C., Berndt, A. et al., Comparative proteomic analysis of normal and tumor stromal cells by tissue on chip based mass spectrometry (toc-MS). *Diagn. Pathol.* 2010, *5*, 10.

[13] Planche, A., Bacac, M., Provero, P., Fusco, C. et al., Identification of prognostic molecular features in the reactive stroma of human breast and prostate cancer. *PloS One* 2011, *6*, e18640.

[14] Singer, C. F., Gschwantler-Kaulich, D., Fink-Retter, A., Haas, C. et al., Differential gene expression profile in breast cancer-derived stromal fibroblasts. *Breast Cancer Res. Treat* 2008, *110*, 273–281.

[15] Volmer, M. W., Stühler, K., Zapatka, M., Schöneck, A. et al., Differential proteome analysis of conditioned media to detect Smad4 regulated secreted biomarkers in colon cancer. *Proteomics* 2005, *5*, 2587–2601.

[16] Hathout, Y., Approaches to the study of the cell secretome. *Expert Rev. Proteomics* 2007, *4*, 239–248.

[17] Koninckx, R., Hensen, K., Daniels, A., Moreels, M. et al., Human bone marrow stem cells co-cultured with neonatal rat cardiomyocytes display limited cardiomyogenic plasticity. *Cytotherapy* 2009, *11*, 778–792.

[18] Kolf, C. M., Cho, E., Tuan, R. S., Mesenchymal stromal cells. Biology of adult mesenchymal stem cells: regulation of niche, self-renewal and differentiation. *Arthritis Res. Ther.* 2007, *9*, 204.

[19] Dominici, M., Blanc, K. L., Mueller, I., Slaper-Cortenbach, I. et al., Minimal criteria for defining multipotent mesenchymal stromal cells. The International Society for Cellular Therapy position statement. *Cytotherapy* 2006, *8*, 315–317.

[20] Majd, H., Wipff, P. J., Buscemi, L., Bueno, M. et al., A novel method of dynamic culture surface expansion improves mesenchymal stem cell proliferation and phenotype. *Stem. Cells* 2009, *27*, 200–209.

[21] De Wever, O., Hendrix, A., De Boeck, A., Westbroek, W. et al., Modeling and quantification of cancer cell invasion through collagen type I matrices. *Int. J. Dev. Biol.* 2010, *54*, 887–896.

[22] Maynard, D. M., Heijnen, H. F. G., Horne, M. K., White, J. G. et al., Proteomic analysis of platelet α-granules using mass spectrometry. *J. Thromb. Haemost.* 2007, *5*, 1945–1955.

[23] Perkins, D. N., Pappin, D. J. C., Creasy, D. M., Cottrell, J. S., Probability-based protein identification by searching sequence databases using mass spectrometry data. *Electrophoresis* 1999, *20*, 3551–3567.

[24] Garbis, S., Lubec, G., Fountoulakis, M., Limitations of current proteomics technologies. *J. Chromatogr. A* 2005, *1077*, 1–18.

[25] Guo, X., Wang, X. F., Signaling cross-talk between TGF-beta/BMP and other pathways. *Cell Res.* 2009, *19*, 71–88.

[26] Narine, K., De Wever, O., Van Valckenborgh, D., Francois, K. et al., Growth factor modulation of fibroblast proliferation, differentiation, and invasion: implications for tissue valve engineering. *Tissue Eng.* 2006, *12*, 2707–2716.

[27] Johnstone, B., Hering, T. M., Caplan, A. I., Goldberg, V. M. et al., In vitro chondrogenesis of bone marrow-derived mesenchymal progenitor cells. *Exp. Cell. Res.* 1998, *238*, 265–272.

[28] Solorio, L. D., Fu, A. S., Hernández-Irizarry, R., Alsberg, E., Chondrogenic differentiation of human mesenchymal stem cell aggregates via controlled release of TGF-β1 from incorporated polymer microspheres. *J. Biomed. Mater Res. A* 2009, *92A*, 1139–1144.

[29] Bauer, M., Su, G., Casper, C., He, R. et al., Heterogeneity of gene expression in stromal fibroblasts of human breast carcinomas and normal breast. *Oncogene* 2010, *29*, 1732–1740.

[30] Orimo, A., Gupta, P. B., Sgroi, D. C., Arenzana-Seisdedos, F. et al., Stromal fibroblasts present in invasive human breast carcinomas promote tumor growth and angiogenesis through elevated SDF-1/CXCL12 secretion. *Cell* 2005, *121*, 335–348.

[31] Verrecchia, F., Chu, M. L., Mauviel, A., Identification of novel TGF-beta/Smad gene targets in dermal fibroblasts using a combined cDNA microarray/promoter transactivation approach. *J. Biol. Chem.* 2001, *276*, 17058–17062.

[32] Bootcov, M. R., Bauskin, A. R., Valenzuela, S. M., Moore, A. G. et al., MIC-1, a novel macrophage inhibitory cytokine, is a divergent member of the TGF-beta superfamily. *Proc. Natl. Acad. Sci. USA* 1997, *94*, 11514–11519.

[33] Zielske, S. P., Livant, D. L., Lawrence, T. S., Radiation increases invasion of gene-modified mesenchymal stem cells into tumors. *Int. J. Radiat. Oncol. Biol. Phys.* 2009, *75*, 843–853.

[34] Saigusa, S., Toiyama, Y., Tanaka, K., Yokoe, T. et al., Cancer-associated fibroblasts correlate with poor prognosis in rectal cancer after chemoradiotherapy. *Int. J. Oncol.* 2011, *38*, 655–663.

[35] Riedl, S., Bodenmuller, H., Hinz, U., Holle, R. et al., Significance of tenascin serum level as tumor marker in primary colorectal carcinoma. *Int. J. Cancer* 1995, *64*, 65–69.

[36] Paulitschke, V., Kunstfeld, R., Mohr, T., Slany, A. et al., Entering a new era of rational biomarker discovery for early detection of melanoma metastases: secretome analysis of associated stroma cells. *J. Proteome Res.* 2009, *8*, 2501–2510.

[37] Sardana, G., Jung, K., Stephan, C., Diamandis, E. P., Proteomic analysis of conditioned media from the PC3, LNCaP, and 22Rv1 prostate cancer cell lines: discovery and validation of candidate prostate cancer biomarkers. *J. Proteome Res.* 2008, *7*, 3329–3338.

[38] Rocco, M., Malorni, L., Cozzolino, R., Palmieri, G. et al., Proteomic profiling of human melanoma metastatic cell line secretomes. *J. Proteome Res.* 2011, *10*, 4703–4714.

[39] Choi, Y. A., Lim, J., Kim, K. M., Acharya, B. et al., Secretome analysis of human BMSCs and identification of SMOC1 as an important ECM protein in osteoblast differentiation. *J. Proteome Res.* 2010, *9*, 2946–2956.

